

PET imaging of epidermal growth factor receptor expression in tumours using ^{89}Zr -labelled ZEGFR:2377 affibody molecules

JAVAD GAROUSI^{1*}, KEN G. ANDERSSON^{2*}, BOGDAN MITRAN³, MARIE-LOUISE PICHL¹, STEFAN STÅHL², ANNA ORLOVA³, JOHN LÖFBLOM² and VLADIMIR TOLMACHEV¹

¹Institute of Immunology, Genetic and Pathology, Uppsala University, SE-75185 Uppsala; ²Division of Protein Technology, KTH Royal Institute of Technology, SE-10691 Stockholm; ³Division of Molecular Imaging, Department of Medicinal Chemistry, Uppsala University, SE-751 83 Uppsala, Sweden

Received November 18, 2015; Accepted December 23, 2015

DOI: 10.3892/ijo.2016.3369

Abstract. Epidermal growth factor receptor (EGFR) is a transmembrane tyrosine kinase receptor, which is overexpressed in many types of cancer. The use of EGFR-targeting monoclonal antibodies and tyrosine-kinase inhibitors improves significantly survival of patients with colorectal, non-small cell lung cancer and head and neck squamous cell carcinoma. Detection of EGFR overexpression provides important prognostic and predictive information influencing management of the patients. The use of radionuclide molecular imaging would enable non-invasive repeatable determination of EGFR expression in disseminated cancer. Moreover, positron emission tomography (PET) would provide superior sensitivity and quantitation accuracy in EGFR expression imaging. Affibody molecules are a new type of imaging probes, providing high contrast in molecular imaging. In the present study, an EGFR-binding affibody molecule (ZEGFR:2377) was site-specifically conjugated with a deferoxamine (DFO) chelator and labelled under mild conditions (room temperature and neutral pH) with a positron-emitting radionuclide ^{89}Zr . The ^{89}Zr -DFO-ZEGFR:2377 tracer demonstrated specific high affinity (160 ± 60 pM) binding to EGFR-expressing A431 epidermoid carcinoma cell line. In mice bearing A431 xenografts, ^{89}Zr -DFO-ZEGFR:2377 demonstrated specific uptake in tumours and EGFR-expressing tissues. The tracer provided tumour uptake of $2.6\pm 0.5\%$ ID/g and tumour-to-blood ratio of 3.7 ± 0.6 at 24 h after injection. ^{89}Zr -DFO-ZEGFR:2377 provides higher tumour-to-organ ratios than anti-EGFR antibody ^{89}Zr -DFO-cetuximab at 48 h after injection. EGFR-expressing tumours were clearly visual-

ized by microPET using ^{89}Zr -DFO-ZEGFR:2377 at both 3 and 24 h after injection. In conclusion, ^{89}Zr -DFO-ZEGFR:2377 is a potential probe for PET imaging of EGFR-expression *in vivo*.

Introduction

Targeting of cancer-associated abnormalities with specific drugs is a promising strategy in treatment of disseminated malignancies. The epidermal growth factor receptor (EGFR) is a transmembrane tyrosine kinase receptor that regulates cell proliferation and survival, but is abnormally expressed and/or activated in many epithelial tumours (1,2). EGFR is a target for several anticancer therapeutics, such as tyrosine kinase inhibitors gefitinib and erlotinib and monoclonal antibodies cetuximab and panitumumab (3).

High level of EGFR expression is associated with poor prognosis in a number of cancers, such as head and neck squamous cell carcinoma (HNSCC) (4), breast (5) and non-small-cell lung cancer (NSCLC) (6). High EGFR expression predicts resistance to neoadjuvant therapy with anthracyclines and taxanes in triple-negative breast cancer (7) and relapse of HNSCC after radiotherapy (8). Overexpression of EGFR can be used for stratification of patients with advanced NSCLC to gefitinib (9,10) and to first-line chemotherapy in combination with cetuximab (11). Patients with a high expression of EGFR in NSCLC might also benefit from the addition of cetuximab to chemoradiotherapy, but cetuximab might be detrimental for patients with low EGFR expression (12). Patients with high EGFR expression in HNSCC may benefit from hyperfractionated accelerated radiotherapy (13). Thus, detection of high EGFR expression levels in malignant tumours may provide important prognostic and predictive information influencing management of the patients.

Currently, EGFR expression level is determined using analyses of biopsy material. However, the biopsy-based methods are invasive and associated with morbidity. Therefore, a limited number of biopsy samples are usually taken. Furthermore, the EGFR expression might change over time due to genetic instability of the cancer and/or in response to therapy (14). An appreciable discrepancy in EGFR expression in primary tumours and corresponding metastases has been documented in colorectal cancer (15,16) and NSCLC (17,18).

Correspondence to: Professor Vladimir Tolmachev, Institute of Immunology, Genetic and Pathology, Uppsala University, Dag Hammarskjölds väg 20, SE-75185 Uppsala, Sweden
E-mail: vladimir.tolmachev@igp.uu.se

*Contributed equally

Key words: epidermal growth factor receptor, affibody molecules, radionuclide imaging, positron emission tomography, zirconium-89, xenografts

There is an unmet clinical need to establish a methodology enabling non-invasive repeatable assessment of EGFR expression during course of disease.

Radionuclide molecular imaging with EGFR-specific agents might be a way to provide repetitive non-invasive assessment of target expression level. Goldenberg and co-workers (19) have demonstrated that the ^{111}In -labeled anti-EGFR antibody 225 (murine predecessor of cetuximab) accumulates in human cancer xenografts in mice proportionally to the EGFR-expression. A clinical study confirmed that ^{111}In -225 can visualize EGFR-expressing tumours in patients (20). The cited study also identified the major obstacle for EGFR visualization *in vivo*, which is the expression of the receptors in multiple normal tissues, foremost in the liver. However, the authors have shown that increasing the injected antibody dose saturates receptors in normal tissues but not in tumours making imaging possible. Still, there are general issues with antibody-based imaging agents, such as a long residence time in circulation and slow penetration into tumours. This results in low tumour-to-blood ratios, translating into low contrast and therefore, a low sensitivity of imaging. Positron-emission tomography (PET) provides better resolution and sensitivity than single photon emission computed tomography (SPECT). Therefore, labelling of anti-EGFR antibodies with long-lived positron emitting radionuclides ^{64}Cu ($T_{1/2}=12.7$ h) (21,22), ^{86}Y ($T_{1/2}=14.7$ h) (23,24), and ^{89}Zr ($T_{1/2}=78.4$ h) (25,26) has been evaluated. While ^{64}Cu and ^{86}Y -labelled antibodies have shown promising results in murine models at 24–48 h, the half-life of these nuclides is too short for clinical translation. The use of the more long-lived ^{89}Zr is probably the only viable option in clinical settings. Still, it would be desirable to have higher contrast than antibodies could provide even if PET is used for imaging.

An alternative to antibodies is the use of a radiolabelled natural ligand of EGFR, epidermal growth factor (EGF) (27–30). This small (6 kDa) protein has much more rapid extravasation rate than bulky (150 kDa) antibodies. Small size results also in a rapid clearance of unbound imaging agent via the kidneys, which is a precondition for high contrast imaging. Raily and co-workers (28) have demonstrated that ^{111}In -EGF provides higher tumour-to-blood ratio than anti-EGFR antibody labelled with the same nuclide. The major issue with the use of EGF as an imaging agent is its strong agonistic action causing nausea, vomiting and hypotension at higher injected doses (27). An ideal agent for EGFR imaging should be as small as EGF but without agonistic properties upon binding to the receptor.

Affibody molecules constitute a rather new class of imaging agents that meet the requirements of small size and absence of agonistic action (31). Affibody molecules are engineered scaffold protein binders, which are originally based on a domain of protein A (32). The use of molecular display techniques enables selection of high-affinity affibody binders to variety of molecular targets (31,32). Due to the small size (7 kDa) and high affinity (low nanomolar or subnanomolar level), affibody molecules is a very promising format of targeting proteins for radionuclide molecular imaging (33,34). In the clinic, affibody molecules have demonstrated feasibility of imaging of HER2-expressing breast cancer metastases with high specificity and sensitivity (35). Earlier, we have reported development

of high-affinity anti-EGFR affibody molecules for the use in radionuclide imaging (36–38). These studies resulted in development of the ZEGFR:2377 affibody molecule that has equal affinity to human and murine EGFR (38). This makes mouse models relevant for preclinical evaluations. In preclinical studies, ^{111}In -DOTA-ZEGFR:2377 provided a tumour-to-blood ratio exceeding the tumour-to-blood ratios of any anti-EGFR monoclonal antibody. However, the use of the radionuclide ^{111}In requires SPECT for imaging. As PET imaging provides better sensitivity of diagnostics, development of an affibody-based agent labelled with a positron emitting nuclide would be desirable.

Previous studies (38) have shown that ^{111}In -DOTA-ZEGFR:2377 provides the highest tumour-to-blood ratio and therefore the best sensitivity at 24 h after injection. Hence, the use of short-lived positron emitting nuclides, such as ^{18}F ($T_{1/2}=109.8$ min) or ^{68}Ga ($T_{1/2}=67.6$ min), for labelling of ZEGFR:2377 would be suboptimal. The use of a more long-lived positron emitter would be desirable. Earlier studies have demonstrated that the use of radiometal labels for anti-EGFR affibody provide better contrast than the use of radiohalogens (37), which excludes the positron-emitting halogen ^{124}I ($T_{1/2}=109.8$ min) as a label. Therefore, a long-lived positron emitter, such as ^{89}Zr ($T_{1/2}=78.4$ h) would be a better choice for labelling of ZEGFR:2377.

The goal of the present study was to evaluate a ^{89}Zr -labelled anti-EGFR ZEGFR:2377 affibody molecule for imaging of EGFR expression in human xenografts in mice and to compare imaging properties of ^{89}Zr ZEGFR:2377 with properties of anti-EGFR antibody ^{89}Zr -cetuximab.

Materials and methods

Material. Zirconium-89 (solution in 1 M oxalic acid) was purchased from Perkin-Elmer (Waltham, MA, USA).

Statistics. Data on cellular uptake and biodistribution were analyzed by unpaired, two-tailed t-test using GraphPad Prism (version 4.00 for Windows GraphPad Software) in order to determine significant differences ($P<0.05$).

Preparation of targeting conjugates. Anti-EGFR ZEGFR:2377 affibody molecule having a single C-terminal cysteine was produced as previously described (38).

For labelling with ^{89}Zr , ZEGFR:2377 was conjugated to a maleimido derivative of deferoxamine (DFO) chelator (Macrocyclics, Dallas, TX, USA). To reduce spontaneously formed intermolecular disulphide bonds, affibody molecules were treated with dithiothreitol (DTT; E. Merck, Darmstadt, Germany). Affibody molecules (2 ml, 2.3 mg/ml in PBS) were mixed with 100 μl 1 M Tris-HCl buffer, pH 8.0, and 63 μl DTT solution (0.5 M in water). The mixture was incubated at 40°C for 30 min. The reduced affibody molecules were then purified and the buffer was changed using a disposable PD-10 column (GE Healthcare, Uppsala, Sweden) pre-equilibrated with 0.2 M ammonium acetate, pH 5.5. The DFO-to-ZEGFR:2377 ratio was optimized to obtain conjugate in high yield. To do this, a 2-, 3-, 5- and 8-fold molar excess of DFO (0.0337 $\mu\text{mole}/\mu\text{l}$ DMSO) was added to the ZEGFR:2377 (0.5 mg in 0.72 ml 0.1 M ammonium acetate buffer, pH 5.5) under gentle shaking,

and incubated for 30 min at 40°C. Unconjugated molecules and excess chelators were separated from the DFO-conjugated affibody molecules on a semi-preparative RP-HPLC column (Zorbax 300SB-C18 9.4x250 mm, 5 µm particle size; Agilent Technologies, Palo Alto, CA, USA) using a gradient from 35-60% B for 18 min at a flow rate of 0.5 ml/min (A: 0.1% trifluoroacetic acid in water, B: 0.1% trifluoroacetic acid in acetonitrile). The analysis was performed using high-performance liquid chromatography and on-line mass spectrometry (HPLC-MS) using an Agilent 1100 LC/MSD system equipped with electrospray ionization and single quadrupole (Agilent Technologies). The analysis was performed using a Zorbax 300SB-C18 2.1x150 mm, 3.5 µm column. Agilent ChemStation Rev. B.02.01 software (Agilent Technologies) was used for analysis and evaluation of HPLC data. The purified conjugate (further designated as DFO-ZEGFR:2377) was freeze-dried.

Cetuximab was conjugated with *p*-isothiocyanatobenzyl-desferrioxamine (Df-Bz-NCS) as previously described (39). The conjugate was purified using a NAP-5 size-exclusion column equilibrated with PBS.

Radiolabeling. DFO-ZEGFR:2377 was labelled with ⁸⁹Zr using a modified method published by Vosjan and co-workers (39). A solution of ⁸⁹Zr (67 µl, 30-40 MBq) was mixed with 30.2 µl 2 M Na₂CO₃, and the mixture was incubated for 3 min. Thereafter, 100 µl 0.5 M HEPES buffer, pH 7.1 was added followed by DFO-ZEGFR:2377 (50 µg dissolved in 240 µl ammonium acetate, pH 5.5) and 234.5 µl 0.5 M HEPES, pH 7.1. The mixture was incubated for 60 min at room temperature. The final purification of ⁸⁹Zr-DFO-ZEGFR:2377 was performed using a NAP-5 size-exclusion column equilibrated with PBS.

For labelling of DFO-cetuximab, a solution of ⁸⁹Zr (7 µl, 4 MBq) was mixed with 3 µl 2 M Na₂CO₃, the mixture was incubated for 3 min and 10 µl 0.5 M HEPES buffer, pH 7.1 was added. DFO-cetuximab (100 µg dissolved in 60 µl ammonium acetate, pH 5.5) and 60 µl 0.5 M HEPES, pH 7.1, were added and the mixture was incubated for 90 min.

Radio-instant thin layer chromatography (radio-ITLC) was used to measure yield, purity and stability of radiolabelled conjugates. ITLC strips (150-771 Dark Green Tec-Control Chromatography strips; Biodex Medical Systems, Shirley, NY, USA) were eluted with 0.2 M citric acid, pH 2.0. An SDS-PAGE analysis was performed [NuPAGE 4-12% Bis-Tris Gel in MES buffer (both from Invitrogen AB Foster City, CA, USA), 200 V constant] to cross-validate the ITLC.

Stability of ⁸⁹Zr-DFO-ZEGFR:2377 was measured in PBS and murine blood plasma up to 24 h. For blood stability studies, freshly labelled ⁸⁹Zr-DFO-ZEGFR:2377 (10 µl) was diluted in a serum sample (240 µl) to a concentration similar to the concentration in blood at the time of injection.

In vitro studies. *In vitro* binding and cellular processing studies were performed using EGFR-expressing A431 epidermoid carcinoma cell line (ATCC; purchased via LGC Promochem, Borås, Sweden). Binding specificity and cellular processing of ⁸⁹Zr-DFO-ZEGFR:2377 were evaluated according to methods previously described (40). To determine binding specificity, A431 cells (3 cell culture dishes) were incubated for 1 h at 37°C with 10 nM ⁸⁹Zr-DFO-ZEGFR:2377. Two sets of control

dishes were pre-treated with 100-fold molar excess of either non-labelled ZEGFR:2377 or cetuximab 5 min before adding 10 nM ⁸⁹Zr-DFO-ZEGFR:2377 and incubated at the same conditions. After 1-h incubation, the incubation media were collected, the cells were detached using trypsin and collected. Radioactivity in cells and incubation media was measured, and percentage of cell-bound radioactivity was measured. Binding specificity of ⁸⁹Zr-DFO-cetuximab was evaluated in the same way.

To determine internalization rate, A431 cells were incubated with 10 nM ⁸⁹Zr-DFO-ZEGFR:2377 at 37°C in a humidified incubator. At 1, 2, 4, 8 and 24 h after incubation start, internalized and membrane-bound radioactivity in a set of three dishes was determined by the acid wash method, as previously described (40). Briefly, the incubation medium was collected, cells were washed by an ice-cold medium and treated with 4 M urea solution in a 0.1 M glycine buffer, pH 2.5, for 5 min on ice. The buffer was collected, the cells were additionally washed with the buffer and the acidic fractions were pooled. Thereafter, the cells were lysed by a treatment with 1 M sodium hydroxide solution (0.5 h at 37°C) for at least 0.5 h. The basic solution containing cell debris with internalized radioactivity was collected. Dishes were additionally washed with sodium hydroxide and alkaline fractions were pooled. Radioactivity of the fractions was measured. Radioactivity in acidic fractions represented membrane-bound tracer, and radioactivity of alkaline fraction presented internalized tracer.

Kinetics of ⁸⁹Zr-DFO-ZEGFR:2377 binding to and dissociation from living A431 cells was measured by using LigandTracer Yellow instrument (Ridgeview Instruments AB, Väinge, Sweden). The data were analyzed using InteractionMap software (Ridgeview Diagnostics AB, Uppsala, Sweden) to calculate association rate, dissociation rate and dissociation constant at equilibrium as previously described (41).

Animal studies. The animal experiments were planned and performed in accordance with the national regulation on laboratory animals' protection and were approved by the Ethics Committee for Animal Research in Uppsala. Euthanasia was performed under Ropmpun/Ketalar anesthesia, and all efforts were made to minimize suffering. Female outbred BALB/c nu/nu mice were purchased from Taconic M&B a/S (Ry, Denmark). At the time of the experiment, the average animal weight was 19±1 g. EGFR-expressing xenografts were established by subcutaneous injection of 10⁷ A431 cells in the right hind leg. The tumours were grown for 12-14 days before the experiment. The animals were randomized into groups of four.

For biodistribution measurements, three groups of mice were intravenously injected with ⁸⁹Zr-DFO-ZEGFR:2377 (20 kBq in 100 µl PBS per mouse). The injected protein dose was adjusted to 40 µg per mouse by non-labelled affibody molecule. One group was euthanized at 3 and another at 24 h after injection, and distribution of radioactivity was measured. To confirm the EGFR specificity of *in vivo* targeting, the receptors in one group of mice were pre-saturated by injection of 400 µg of non-labelled ZEGFR:2377 40 min before injection of ⁸⁹Zr-DFO-ZEGFR:2377. Biodistribution in this group of mice was measured at 3 h after injection. For comparison, one group of mice was injected with ⁸⁹Zr-DFO-cetuximab (30 kBq/50 µg in 100 µl PBS per mouse) and the biodistribu-

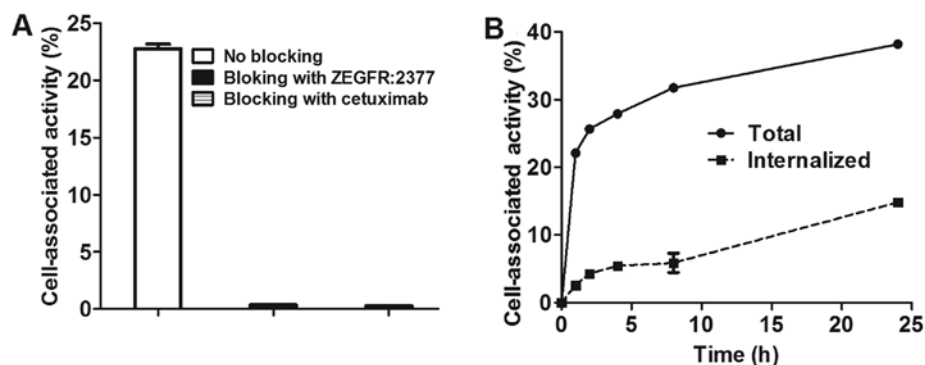


Figure 1. (A) *In vitro* specificity of ^{89}Zr -DFO-ZEGFR:2377 binding to EGFR-expressing A431 cells. (B) Cellular processing of ^{89}Zr -DFO-ZEGFR:2377 by A431 cells during continuous incubation.

tion was measured at 48 h after injected. After euthanasia, blood and organ samples were collected and weighed, and their radioactivity was measured. Tissue uptake (decay corrected) was calculated as percent of injected dose per gram (% ID/g).

Whole body positron emission tomography (PET)/computed tomography (CT) scans of the mice injected with ^{89}Zr -DFO-Z2377 (45 μg , 4.6 MBq) were performed in TriumphTM tri-modality system (TriFoil Imaging, Inc., Northridge, CA, USA) at 3 and 24 h p.i. The animals were sacrificed by CO_2 asphyxiation immediately before being placed in the camera. The urinary bladder was excised post-mortem due to its proximity to tumor xenografts and kidneys. The PET scans were conducted for 30 min followed by CT examination at the following parameters: field of view (FOV), 8 cm; magnification, 1.48; one frame and 512 projections for 2.13 min. CT raw files were reconstructed by filter back projection (FBP). PET data were reconstructed into a static image using OSEM-3D (20 iterations). The scatter and attenuation correction were performed using their respective CT data. PET and CT files were analyzed using PMOD v3.508 (PMOD Technologies Ltd., Zurich, Switzerland). Coronal PET-CT images are presented as maximum intensity projections (MIP) in RGB color scale.

Results

Preparation of targeting conjugates. Increase of chelator-to-protein molar ratio from 3:1 to 5:1 improved the conjugation yield from 81 to 93%. Further increase of the chelator-to-protein molar ratio to 8:1 did not improve the conjugation (yield of 93%). Semipreparative HPLC enabled efficient separation of DFO-ZEGFR:2377 from unconjugated ZEGFR:2377. HPLC analysis demonstrated that the purity of DFO-ZEGFR:2377 was >95%. The mass spectrometry analysis showed an excellent agreement between the molecular mass of DFO-ZEGFR:2377 with the theoretical value (expected 8102.8 Da, observed 8103 Da).

Radiolabelling. Labelling of DFO-ZEGFR:2377 with ^{89}Zr provided yield of $99\pm 1\%$. Purification using a disposable NAP-5 size-exclusion column provided purity of 100%. The identity of conjugates was confirmed by radio-SDS-PAGE. There was no measurable release of ^{89}Zr from ^{89}Zr -DFO-ZEGFR:2377 during incubation in PBS (Table I). A minimum release (<3%) was observed in murine blood plasma after incubation for 24 h.

Table I. Stability of ^{89}Zr -DFO-ZEGFR:2377 in PBS and murine blood plasma.

	Protein-associated radioactivity, %			
	1 h	2 h	4 h	24 h
PBS	100 \pm 0	100 \pm 0	100 \pm 0	100 \pm 0
Plasma	100 \pm 0	100 \pm 0	100 \pm 0	98.5 \pm 1.5

Data are presented as an average from two measurement \pm maximum error.

***In vitro* studies.** Data concerning specificity of ^{89}Zr -DFO-ZEGFR:2377 binding to EGFR-expressing A431 cells are presented in Fig. 1A. Pre-saturation of EGFR on A431 cells with an excess of both non-labeled ZEGFR:2377 and cetuximab caused a highly significant ($P < 1 \times 10^{-5}$) reduction of ^{89}Zr -DFO-ZEGFR:2377 binding to the cells. This demonstrates saturability of binding and proves that the binding of the conjugate to EGFR-expressing cells is receptor-mediated. Similarly, specificity of ^{89}Zr -DFO-cetuximab binding to A431 cells was confirmed (data not shown).

Data concerning cellular processing of ^{89}Zr -DFO-ZEGFR:2377 are presented in Fig. 1B. The internalization of ^{89}Zr -DFO-ZEGFR:2377 by A431 cells was relatively slow. The internalized fraction was $\sim 20\%$ after 4-h incubation and $\sim 40\%$ after 24 h.

A representative LigandTracer sensorgram of ^{89}Zr -DFO-ZEGFR:2377 binding to and dissociation from living A431 cells is presented in Fig. 2. The interaction of ^{89}Zr -DFO-ZEGFR:2377 was characterized by rapid binding (association rate of $1.95 \pm 0.45 \times 10^5$ 1/M x s) and slow dissociation (dissociation rate of $3.3 \pm 1.2 \times 10^{-5}$ 1/s). This provided a very high affinity. The dissociation constant (K_D) of ^{89}Zr -labelled DFO-ZEGFR:2377 interaction with A431 cells was 160 ± 60 pM.

Animal studies. The results of an *in vivo* specificity test are presented in Fig. 3. Pre-saturation of EGFR with a large excess of non-labelled affibody molecule caused a significant ($P < 0.0005$) reduction in tumour uptake. Radioactivity uptake was also significantly ($P < 0.05$) reduced in EGFR-expressing tissues, such as liver, salivary gland and lung. There was

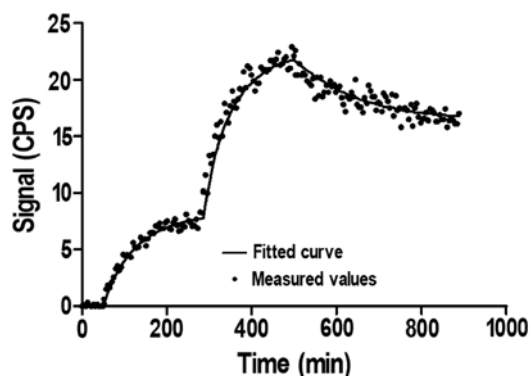


Figure 2. Representative LignadTracer sensorgram of ^{89}Zr -DFO-ZEGFR:2377 binding to EGFR-expressing A431 cells. Uptake curves were recorded at 0.33 and 1 nM.

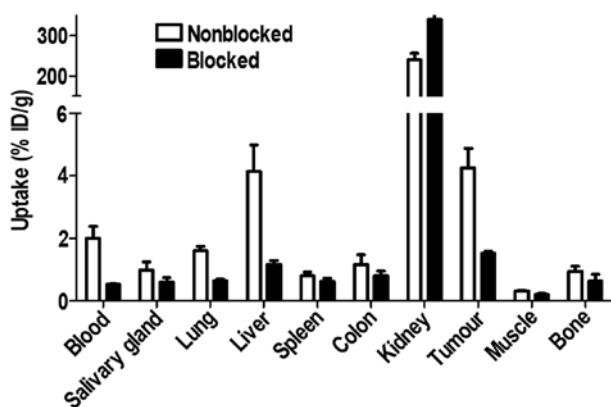


Figure 3. Specificity of ^{89}Zr -DFO-ZEGFR:2377 uptake in A431 xenografts and EGFR-expressing organs in mice at 3 h after injection. In the blocked group, receptors were saturated by pre-injection of large excess of non-labelled affibody molecules.

also a significant reduction of uptake in blood and muscle. Radioactivity uptake in kidneys was increased in the blocked group.

Comparison of ^{89}Zr -DFO-ZEGFR:2377 biodistribution at 3 and 24 h and ^{89}Zr -DFO-cetuximab biodistribution in nude mice bearing EGFR-expressing xenografts is presented in Fig. 4. ^{89}Zr -DFO-ZEGFR:2377 demonstrated relatively rapid blood clearance. Already at 3 h after injection, the blood concentration was $2.0 \pm 0.4\%$ ID/g. Low radioactivity uptake in gastrointestinal tract ($2.5 \pm 0.4\%$ ID pre-whole sample, including content) suggested that hepatobiliary excretion played a minor role in clearance of ^{89}Zr -DFO-ZEGFR:2377. On the contrary, the high kidney uptake suggested that ^{89}Zr -DFO-ZEGFR:2377 underwent a rapid glomerular filtration followed by renal re-absorption, which is typical for affibody molecules. The tumour uptake ($4.3 \pm 0.6\%$ ID/g) exceeded the uptake in other organs and tissues except for liver ($4.1 \pm 0.9\%$ ID/g) and kidneys. At 24 h after injection, the blood concentration of ^{89}Zr -DFO-ZEGFR:2377 decreased nearly 3-fold, from $2.0 \pm 0.3\%$ ID/g to $0.70 \pm 0.07\%$ ID/g. There was no significant decrease of uptake in salivary gland, spleen, colon, and kidney between 3 and 24 h after injection. There was significant ($P < 0.05$) decrease of ^{89}Zr uptake in the tumour, or in lung, liver and muscle. The ^{89}Zr uptake in bone increased at 24 h.

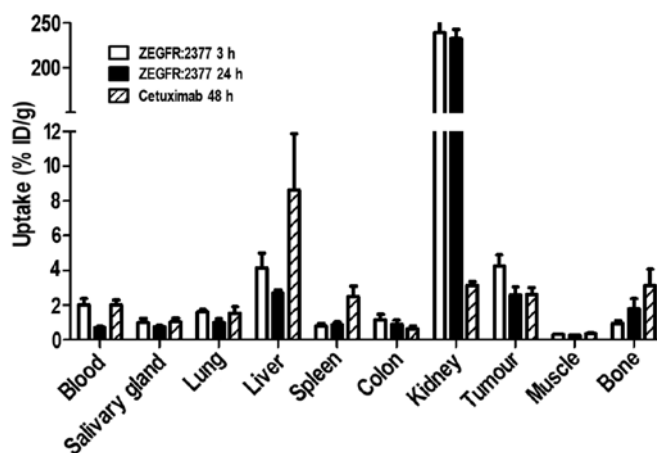


Figure 4. Biodistribution of ^{89}Zr -DFO-Z2377 and ^{89}Zr -DFO-cetuximab in BALB/C nu/nu mice bearing EGFR-expressing A431 xenografts.

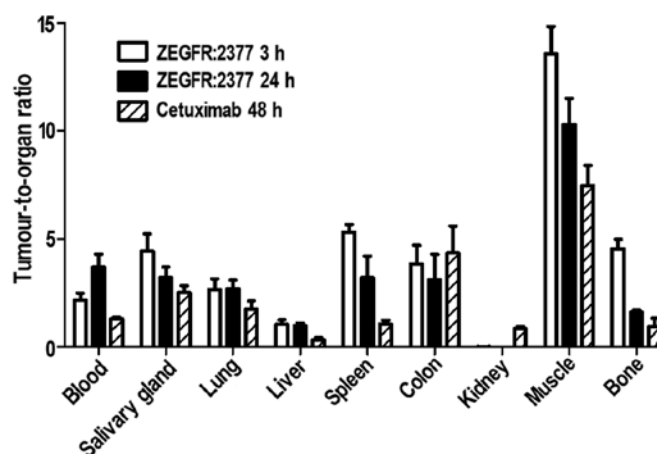


Figure 5. Tumour-to-organ ratios of ^{89}Zr -DFO-Z2377 and ^{89}Zr -DFO-cetuximab in BALB/C nu/nu mice bearing EGFR-expressing A431 xenografts.

Biodistribution of ^{89}Zr -DFO-cetuximab was measured at 48 h after injection, i.e. an optimal time-point for imaging using radiolabelled monoclonal antibodies. At this time-point, the tumour uptake of ^{89}Zr -DFO-cetuximab was at the same level as uptake of ^{89}Zr -DFO-ZEGFR:2377 at 24 h after injection. However, uptake of ^{89}Zr -DFO-cetuximab was significantly higher in blood, salivary gland, lung, liver, spleen and muscles. The use of monoclonal antibody provided significantly lower uptake in kidneys.

Tumour-to-organ ratios for ^{89}Zr -labelled tracers, which determine contrast and therefore sensitivity of imaging, are presented in Fig. 5. At both time-points, ^{89}Zr -DFO-ZEGFR:2377 provided significantly higher tumour-to-organ ratios than ^{89}Zr -DFO-cetuximab except from the tumour-to-kidney ratio and, at 4 h after injection, the tumour-to-salivary gland ratio. At 24 h after injection, the tumour-to-blood ratio for ^{89}Zr -DFO-ZEGFR:2377 (3.7 ± 0.6) was 1.7-fold higher than at 3 h after injection. At the same time, tumour-to-muscle ratio was reduced 1.3-fold, tumour-to-bone ratio 2.8-fold and tumour-to-spleen ratio 1.4-fold. There was no significant difference in tumour-to-organ ratios for other tissues.

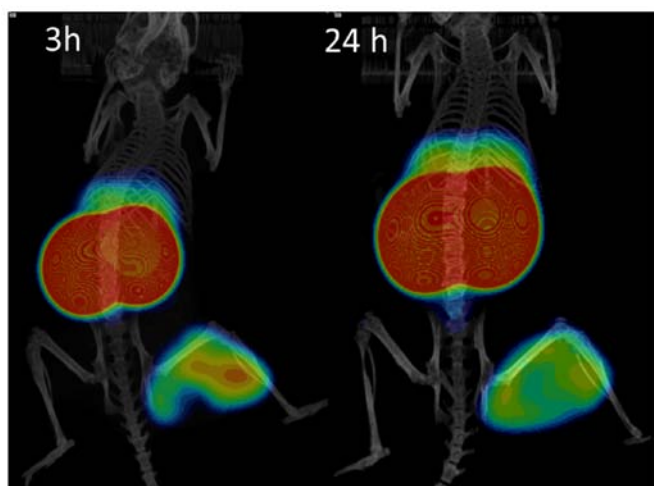


Figure 6. Imaging of EGFR-expressing A431 xenografts in BALB/C nu/nu mice using ^{89}Zr -DFO-ZEGFR:2377 at 3 and 24 h after injection. Coronal PET-CT images are presented as maximum intensity projections (MIP) in RGB colour scale.

MicroPET imaging of EGFR expression in mice bearing A431 xenografts using ^{89}Zr -DFO-ZEGFR:2377 is presented in Fig. 6. The images were in a good agreement with the biodistribution data. The highest concentration of radioactivity was in kidneys. Liver showed also a prominent uptake of radioactivity. Tumours on right hind legs were clearly visualized. The tumour uptake was at the same level as in the liver (somewhat higher at 3 h after injection) and noticeably higher than uptake in any other tissue. The image at 3 h provided somewhat better contrast towards bones.

Discussion

PET as an imaging modality has traditionally been associated with applications using radiolabelled small molecules as imaging agents and protein-based imaging agents were typically applied in SPECT imaging. However, the intrinsic advantages of PET, such as higher sensitivity, better resolution and superior quantification accuracy caused an increased interest in the labelling of proteinaceous imaging probes with positron-emitting nuclides and their use for PET imaging (42). The short-lived positron-emitting nuclides, such as ^{18}F ($T_{1/2}=109.8$ min) or ^{68}Ga ($T_{1/2}=67.6$ min), are perfect labels for small peptides providing high contrast already a few hours after injection (42). These nuclides have been successfully used for labelling of e.g. anti-HER2 and anti-PDGFR affibody molecules (43-45). However, anti-EGFR affibody molecules have unusually slow blood clearance. This might be associated with their slow internalisation after binding to EGFR in normal tissues (38). Clearance from blood causes dissociation of the reversibly bound tracer from EGFR-expressing tissues and its release back to blood circulation. Thus, the tumour-to-blood ratio for ^{18}F -labelled anti-EGFR ZEGFR:1907 affibody molecules was around 2 within the time window for this short-lived nuclide, although three different labelling approaches were tested (46,47). The low tumour-to-blood ratio translates into low overall contrast and compromises sensitivity of imaging diagnostics. Previous studies have shown that the

tumour-to-blood ratio for ^{111}In -DOTA-ZEGFR:2377 affibody molecule is significantly higher at 24 than at 4 h after injection. However, next-day-imaging requires a more long-lived positron-emitting label.

Radionuclide ^{89}Zr seems suitable for labelling of affibody molecules for PET imaging on the next day after injection. This nuclide has been successfully used for labelling of several antibodies for preclinical (25,26,48,49) and clinical (50,51) PET imaging. Derivatives of deferoxamine (DFO) chelator provide attachment of ^{89}Zr to targeting proteins under mild conditions (room temperature, neutral pH) with adequate stability (52). ^{89}Zr is currently commercially available.

In this study, a maleimido derivative of DFO was site-specifically conjugated to a unique cysteine at the C-terminus of ZEGFR:2377 affibody molecules, providing a homogeneous conjugate. DFO-ZEGFR:2377 was efficiently labelled with ^{89}Zr . The conjugate was stable both in PBS and in murine plasma during incubation up to 24 h (Table I). The ^{89}Zr -DFO-ZEGFR:2377 affibody tracer demonstrated specific binding to EGFR-expressing cells (Fig. 1) and high affinity (160 ± 60 pM, as measured by LigandTracer). The slow internalization of ^{89}Zr -DFO-ZEGFR:2377 by A431 cells (Fig. 1) was consistent with earlier findings for ^{111}In -DOTA-ZEGFR:2377 (38). *In vivo*, ^{89}Zr -DFO-ZEGFR:2377 bound specifically to EGFR-expressing xenografts and EGFR-expressing murine organs at 3 h after injection (Fig. 3). Saturation of uptake in normal tissues resulted in lower release of the conjugate back to circulation, which resulted in lower concentration of radioactivity in blood and muscles (Fig. 3). In addition, non-bound ^{89}Zr -DFO-ZEGFR:2377 was cleared from blood and re-absorbed in the kidneys, which resulted in higher kidney uptake after blocking (Fig. 3). The increased uptake in the kidneys upon blocking suggests that the renal uptake of ^{89}Zr -DFO-ZEGFR:2377 is not EGFR-mediated. Most likely, the renal re-absorptions of ^{89}Zr -DFO-ZEGFR:2377 is mediated by one of the 'scavenger receptor' systems that is responsible for recovery of proteins from primary urine (53). Although the high renal re-absorption is a common feature of affibody molecules (34), its exact mechanism is still not known. It has to be noted that the high renal uptake does not prevent visualization of tumours in close vicinity of the kidneys. For example, a HER2-expressing adrenal metastasis has been clearly visualized by the anti-HER2 ^{111}In -ABY-025 affibody molecule during a clinical study (35), although the renal uptake of this tracer was as high as the uptake of ^{89}Zr -DFO-ZEGFR:2377 in preclinical studies (54).

At 24 h after injection, the uptake of ^{89}Zr -DFO-ZEGFR:2377 in tumours and majority of tissues was reduced compared to uptake at 3 h (Fig. 4). The only exception was bone, where the uptake of ^{89}Zr was higher at 24 h after injection. This is consistent with the data for ^{89}Zr -labelled antibodies, which also demonstrated increase of the bone uptake at later time-points (48,52). This might be an indication of release of the radionuclide from the conjugate *in vivo* (52). As ^{89}Zr -DFO-ZEGFR:2377 was stable in the blood plasma *ex vivo* (Table I), we can suppose that the release takes place during catabolism in excretory organs and EGFR-expressing tissues. As the decrease of tumour uptake was slower than blood clearance, the tumour-to-blood ratio significantly ($P<0.05$) increased from 2.2 ± 0.3 to 3.7 ± 0.6 , leading to increased overall imaging

contrast. The EGFR-expressing xenografts were clearly visualized at both 3 and 24 h after injection (Fig. 6).

For comparison, we investigated targeting of EGFR-expressing xenografts using ^{89}Zr -labelled anti-EGFR antibody cetuximab. The biodistribution of ^{89}Zr -DFO-cetuximab was measured at 48 h after injection because the literature data (25) suggest that this time-point is optimal for imaging of A431 xenografts, as there was neither significant increase of tumour uptake nor decrease of blood concentration at later time-points. Our data were in a good agreement with the data published by Aerts and co-workers (25) as the difference was within the measurement accuracy. At the optimal time-point, the tumour uptake of ^{89}Zr -DFO-cetuximab ($2.6\pm 0.4\%$ ID/g) was at the same level as uptake of ^{89}Zr -DFO-ZEGFR:2377 at 24 h after injection ($2.6\pm 0.5\%$ ID/g) and was significantly lower than uptake at 3 h after injection ($4.3\pm 0.6\%$ ID/g). The normal organ uptake of ^{89}Zr -DFO-cetuximab at 48 h was at the same level or higher than uptake of ^{89}Zr -DFO-ZEGFR:2377 at 3 h after injection (Fig. 4). As a result, ^{89}Zr -DFO-ZEGFR:2377 provided at both time-points significantly higher tumour-to-organ ratios than ^{89}Zr -DFO-cetuximab for all organs except from kidneys (Fig. 5). Thus, PET imaging using ^{89}Zr -DFO-ZEGFR:2377 should provide better contrast and, therefore, sensitivity than using ^{89}Zr -DFO-cetuximab. The imaging could be performed earlier after injection, which is an additional clinical advantage.

In conclusion, labelling of anti-EGFR ZEGFR:2377 antibody molecule with the long-lived positron emitting radionuclide ^{89}Zr provides a probe capable of specific PET imaging of EGFR expression in malignant tumours. ^{89}Zr -DFO-ZEGFR:2377 provides higher tumour-to-organ ratios than the anti-EGFR antibody, cetuximab. This should ensure higher sensitivity in clinical imaging.

Acknowledgements

The present study was financially supported by grants from the Swedish Research Council (Vetenskapsrådet) and the Swedish Cancer Society (Cancerfonden).

References

- Mendelsohn J and Baselga J: Epidermal growth factor receptor targeting in cancer. *Semin Oncol* 33: 369-385, 2006.
- Scaltriti M and Baselga J: The epidermal growth factor receptor pathway: A model for targeted therapy. *Clin Cancer Res* 12: 5268-5272, 2006.
- Goffin JR and Zbuk K: Epidermal growth factor receptor: Pathway, therapies, and pipeline. *Clin Ther* 35: 1282-1303, 2013.
- Ang KK, Andratschke NH and Milas L: Epidermal growth factor receptor and response of head-and-neck carcinoma to therapy. *Int J Radiat Oncol Biol Phys* 58: 959-965, 2004.
- Tsutsui S, Kataoka A, Ohno S, Murakami S, Kinoshita J and Hachitanda Y: Prognostic and predictive value of epidermal growth factor receptor in recurrent breast cancer. *Clin Cancer Res* 8: 3454-3460, 2002.
- Selvaggi G, Novello S, Torri V, Leonardo E, De Giuli P, Borasio P, Mossetti C, Ardissoni F, Lausi P and Scagliotti GV: Epidermal growth factor receptor overexpression correlates with a poor prognosis in completely resected non-small-cell lung cancer. *Ann Oncol* 15: 28-32, 2004.
- Humbert O, Riedinger JM, Charon-Barra C, Berriolo-Riedinger A, Desmoulins I, Lorgis V, Kanoun S, Coutant C, Fumoleau P, Cochet A and Brunotte F: Identification of biomarkers including ^{18}F FDG-PET/CT for early prediction of response to neoadjuvant chemotherapy in triple negative breast cancer. *Clin Cancer Res* 21: 5460-5468, 2015.
- Ang KK, Berkey BA, Tu X, Zhang HZ, Katz R, Hammond EH, Fu KK and Milas L: Impact of epidermal growth factor receptor expression on survival and pattern of relapse in patients with advanced head and neck carcinoma. *Cancer Res* 62: 7350-7356, 2002.
- Cappuzzo F, Hirsch FR, Rossi E, Bartolini S, Ceresoli GL, Bemis L, Haney J, Witt S, Danenberg K, Domenichini I, *et al*: Epidermal growth factor receptor gene and protein and gefitinib sensitivity in non-small-cell lung cancer. *J Natl Cancer Inst* 97: 643-655, 2005.
- Hirsch FR, Varella-Garcia M, Bunn PA Jr, Franklin WA, Dziadziuszko R, Thatcher N, Chang A, Parikh P, Pereira JR, Ciuleanu T, *et al*: Molecular predictors of outcome with gefitinib in a phase III placebo-controlled study in advanced non-small-cell lung cancer. *J Clin Oncol* 24: 5034-5042, 2006.
- Pirker R, Pereira JR, von Pawel J, Krzakowski M, Ramlau R, Park K, de Marinis F, Eberhardt WE, Paz-Ares L, Störkel S, *et al*: EGFR expression as a predictor of survival for first-line chemotherapy plus cetuximab in patients with advanced non-small-cell lung cancer: Analysis of data from the phase 3 FLEX study. *Lancet Oncol* 13: 33-42, 2012.
- Bradley JD, Paulus R, Komaki R, Masters G, Blumenschein G, Schild S, Bogart J, Hu C, Forster K, Magliocco A, *et al*: Standard-dose versus high-dose conformal radiotherapy with concurrent and consolidation carboplatin plus paclitaxel with or without cetuximab for patients with stage IIIA or IIIB non-small-cell lung cancer (RTOG 0617): A randomised, two-by-two factorial phase 3 study. *Lancet Oncol* 16: 187-199, 2015.
- Bentzen SM, Atasoy BM, Daley FM, Dische S, Richman PI, Saunders MI, Trott KR and Wilson GD: Epidermal growth factor receptor expression in pretreatment biopsies from head and neck squamous cell carcinoma as a predictive factor for a benefit from accelerated radiation therapy in a randomized controlled trial. *J Clin Oncol* 23: 5560-5567, 2005.
- Vignot S, Besse B, André F, Spano JP and Soria JC: Discrepancies between primary tumor and metastasis: A literature review on clinically established biomarkers. *Crit Rev Oncol Hematol* 84: 301-313, 2012.
- Yarom N, Marginean C, Moyana T, Gorn-Hondermann I, Birnboim HC, Marginean H, Auer RC, Vickers M, Asmis TR, Maroun J, *et al*: EGFR expression variance in paired colorectal cancer primary and metastatic tumors. *Cancer Biol Ther* 10: 416-421, 2010.
- Wei Q, Shui Y, Zheng S, Wester K, Nordgren H, Nygren P, Glimelius B and Carlsson J: EGFR, HER2 and HER3 expression in primary colorectal carcinomas and corresponding metastases: Implications for targeted radionuclide therapy. *Oncol Rep* 25: 3-11, 2011.
- Gomez-Roca C, Raynaud CM, Penault-Llorca F, Mercier O, Commo F, Morat L, Sabatier L, Dartevelle P, Taranchon E, Besse B, *et al*: Differential expression of biomarkers in primary non-small cell lung cancer and metastatic sites. *J Thorac Oncol* 4: 1212-1220, 2009.
- Italiano A, Vandenbos FB, Otto J, Mouroux J, Fontaine D, Marcy PY, Cardot N, Thyss A and Pedeutour F: Comparison of the epidermal growth factor receptor gene and protein in primary non-small-cell-lung cancer and metastatic sites: Implications for treatment with EGFR-inhibitors. *Ann Oncol* 17: 981-985, 2006.
- Goldenberg A, Masui H, Divgi C, Kamrath H, Pentlow K and Mendelsohn J: Imaging of human tumor xenografts with an indium-111-labeled anti-epidermal growth factor receptor monoclonal antibody. *J Natl Cancer Inst* 81: 1616-1625, 1989.
- Divgi CR, Welt S, Kris M, Real FX, Yeh SD, Gralla R, Merchant B, Schweighart S, Unger M, Larson SM, *et al*: Phase I and imaging trial of indium 111-labeled anti-epidermal growth factor receptor monoclonal antibody 225 in patients with squamous cell lung carcinoma. *J Natl Cancer Inst* 83: 97-104, 1991.
- Cai W, Chen K, He L, Cao Q, Koong A and Chen X: Quantitative PET of EGFR expression in xenograft-bearing mice using ^{64}Cu -labeled cetuximab, a chimeric anti-EGFR monoclonal antibody. *Eur J Nucl Med Mol Imaging* 34: 850-858, 2007.
- Ping Li W, Meyer LA, Capretto DA, Sherman CD and Anderson CJ: Receptor-binding, biodistribution, and metabolism studies of ^{64}Cu -DOTA-cetuximab, a PET-imaging agent for epidermal growth-factor receptor-positive tumors. *Cancer Biother Radiopharm* 23: 158-171, 2008.

23. Nayak TK, Garmestani K, Baidoo KE, Milenic DE and Brechbiel MW: Preparation, biological evaluation, and pharmacokinetics of the human anti-*HER1* monoclonal antibody panitumumab labeled with ⁸⁶Y for quantitative PET of carcinoma. *J Nucl Med* 51: 942-950, 2010.
24. Nayak TK, Garmestani K, Milenic DE and Brechbiel MW: PET and MRI of metastatic peritoneal and pulmonary colorectal cancer in mice with human epidermal growth factor receptor 1-targeted ⁸⁹Zr-labeled panitumumab. *J Nucl Med* 53: 113-120, 2012.
25. Aerts HJ, Dubois L, Perk L, Vermaelen P, van Dongen GA, Wouters BG and Lambin P: Disparity between in vivo EGFR expression and ⁸⁹Zr-labeled cetuximab uptake assessed with PET. *J Nucl Med* 50: 123-131, 2009.
26. Chang AJ, De Silva RA and Lapi SE: Development and characterization of ⁸⁹Zr-labeled panitumumab for immuno-positron emission tomographic imaging of the epidermal growth factor receptor. *Mol Imaging* 12: 17-27, 2013.
27. Cuartero-Plaza A, Martínez-Miralles E, Rosell R, Vadell-Nadal C, Farré M and Real FX: Radiolocalization of squamous lung carcinoma with ¹³¹I-labeled epidermal growth factor. *Clin Cancer Res* 2: 13-20, 1996.
28. Reilly RM, Kiarash R, Sandhu J, Lee YW, Cameron RG, Hendlar A, Vallis K and Gariépy J: A comparison of EGF and MAb 528 labeled with ¹¹¹In for imaging human breast cancer. *J Nucl Med* 41: 903-911, 2000.
29. Velikyán I, Sundberg AL, Lindhe O, Höglund AU, Eriksson O, Werner E, Carlsson J, Bergström M, Långström B and Tolmachev V: Preparation and evaluation of ⁶⁸Ga-DOTA-hEGF for visualization of EGFR expression in malignant tumors. *J Nucl Med* 46: 1881-1888, 2005.
30. Li W, Niu G, Lang L, Guo N, Ma Y, Kiesewetter DO, Backer JM, Shen B and Chen X: PET imaging of EGF receptors using [¹⁸F] FBEM-EGF in a head and neck squamous cell carcinoma model. *Eur J Nucl Med Mol Imaging* 39: 300-308, 2012.
31. Löfblom J, Feldwisch J, Tolmachev V, Carlsson J, Ståhl S and Frejd FY: Affibody molecules: Engineered proteins for therapeutic, diagnostic and biotechnological applications. *FEBS Lett* 584: 2670-2680, 2010.
32. Nygren PA: Alternative binding proteins: Affibody binding proteins developed from a small three-helix bundle scaffold. *FEBS J* 275: 2668-2676, 2008.
33. Ahlgren S and Tolmachev V: Radionuclide molecular imaging using Affibody molecules. *Curr Pharm Biotechnol* 11: 581-589, 2010.
34. Feldwisch J and Tolmachev V: Engineering of affibody molecules for therapy and diagnostics. *Methods Mol Biol* 899: 103-126, 2012.
35. Sörensen J, Sandberg D, Sandström M, Wennborg A, Feldwisch J, Tolmachev V, Åström G, Lubberink M, Garske-Román U, Carlsson J, *et al*: First-in-human molecular imaging of HER2 expression in breast cancer metastases using the ¹¹¹In-ABY-025 affibody molecule. *J Nucl Med* 55: 730-735, 2014.
36. Friedman M, Orlova A, Johansson E, Eriksson TL, Höiden-Guthenberg I, Tolmachev V, Nilsson FY and Ståhl S: Directed evolution to low nanomolar affinity of a tumor-targeting epidermal growth factor receptor-binding affibody molecule. *J Mol Biol* 376: 1388-1402, 2008.
37. Tolmachev V, Friedman M, Sandström M, Eriksson TL, Rosik D, Hodik M, Ståhl S, Frejd FY and Orlova A: Affibody molecules for epidermal growth factor receptor targeting in vivo: Aspects of dimerization and labeling chemistry. *J Nucl Med* 50: 274-283, 2009.
38. Tolmachev V, Rosik D, Wällberg H, Sjöberg A, Sandström M, Hansson M, Wennborg A and Orlova A: Imaging of EGFR expression in murine xenografts using site-specifically labelled anti-EGFR ¹¹¹In-DOTA-Z_{EGFR:2377} affibody molecule: aspect of the injected tracer amount. *Eur J Nucl Med Mol Imaging* 37: 613-622, 2010.
39. Vosjan MJ, Perk LR, Visser GW, Budde M, Jurek P, Kiefer GE and van Dongen GA: Conjugation and radiolabeling of monoclonal antibodies with zirconium-89 for PET imaging using the bifunctional chelate p-isothiocyanatobenzyl-desferrioxamine. *Nat Protoc* 5: 739-743, 2010.
40. Malmberg J, Tolmachev V and Orlova A: Imaging agents for *in vivo* molecular profiling of disseminated prostate cancer-targeting EGFR receptors in prostate cancer: comparison of cellular processing of [¹¹¹In]-labeled affibody molecule Z_{EGFR:2377} and cetuximab. *Int J Oncol* 38: 1137-1143, 2011.
41. Barta P, Malmberg J, Melicharova L, Strandgård J, Orlova A, Tolmachev V, Laznickek M and Andersson K: Protein interactions with HER-family receptors can have different characteristics depending on the hosting cell line. *Int J Oncol* 40: 1677-1682, 2012.
42. Tolmachev V and Stone-Elander S: Radiolabelled proteins for positron emission tomography: Pros and cons of labelling methods. *Biochim Biophys Acta* 1800: 487-510, 2010.
43. Altai M, Strand J, Rosik D, Selvaraju RK, Eriksson Karlström A, Orlova A and Tolmachev V: Influence of nuclides and chelators on imaging using affibody molecules: Comparative evaluation of recombinant affibody molecules site-specifically labeled with ⁶⁸Ga and ¹¹¹In via maleimido derivatives of DOTA and NODAGA. *Bioconjug Chem* 24: 1102-1109, 2013.
44. Heskamp S, Laverman P, Rosik D, Boschetti F, van der Graaf WT, Oyen WJ, van Laarhoven HW, Tolmachev V and Boerman OC: Imaging of human epidermal growth factor receptor type 2 expression with ¹⁸F-labeled affibody molecule Z_{HER2:2395} in a mouse model for ovarian cancer. *J Nucl Med* 53: 146-153, 2012.
45. Strand J, Varasteh Z, Eriksson O, Abrahmsen L, Orlova A and Tolmachev V: Gallium-68-labeled affibody molecule for PET imaging of PDGFRβ expression in vivo. *Mol Pharm* 11:3 957-3964, 2014.
46. Miao Z, Ren G, Liu H, Qi S, Wu S and Cheng Z: PET of EGFR expression with an ¹⁸F-labeled affibody molecule. *J Nucl Med* 53: 1110-1118, 2012.
47. Su X, Cheng K, Jeon J, Shen B, Venturin GT, Hu X, Rao J, Chin FT, Wu H and Cheng Z: Comparison of two site-specifically ¹⁸F-labeled affibodies for PET imaging of EGFR positive tumors. *Mol Pharm* 11: 3947-3956, 2014.
48. Dijkers EC, Kosterink JG, Rademaker AP, Perk LR, van Dongen GA, Bart J, de Jong JR, de Vries EG and Lub-de Hooge MN: Development and characterization of clinical-grade ⁸⁹Zr-trastuzumab for HER2/neu immunoPET imaging. *J Nucl Med* 50: 974-981, 2009.
49. Terwisscha van Scheltinga AG, Lub-de Hooge MN, Abiraj K, Schröder CP, Pot L, Bossenmaier B, Thomas M, Hölzlwimmer G, Friess T, Kosterink JG, *et al*: ImmunoPET and biodistribution with human epidermal growth factor receptor 3 targeting antibody ⁸⁹Zr-RG7116. *MAbs* 6: 1051-1058, 2014.
50. Dijkers EC, Oude Munnink TH, Kosterink JG, Brouwers AH, Jager PL, de Jong JR, van Dongen GA, Schröder CP, Lub-de Hooge MN and de Vries EG: Biodistribution of ⁸⁹Zr-trastuzumab and PET imaging of HER2-positive lesions in patients with metastatic breast cancer. *Clin Pharmacol Ther* 87: 586-592, 2010.
51. Oosting SF, Brouwers AH, van Es SC, Nagengast WB, Oude Munnink TH, Lub-de Hooge MN, Hollema H, de Jong JR, de Jong IJ, de Haas S, *et al*: ⁸⁹Zr-bevacizumab PET visualizes heterogeneous tracer accumulation in tumor lesions of renal cell carcinoma patients and differential effects of antiangiogenic treatment. *J Nucl Med* 56: 63-69, 2015.
52. Fischer G, Seibold U, Schirmacher R, Wängler B and Wängler C: ⁸⁹Zr, a radiometal nuclide with high potential for molecular imaging with PET: Chemistry, applications and remaining challenges. *Molecules* 18: 6469-6490, 2013.
53. Vegt E, de Jong M, Wetzels JF, Masereeuw R, Melis M, Oyen WJ, Gotthardt M and Boerman OC: Renal toxicity of radiolabeled peptides and antibody fragments: Mechanisms, impact on radionuclide therapy, and strategies for prevention. *J Nucl Med* 51: 1049-1058, 2010.
54. Ahlgren S, Orlova A, Wällberg H, Hansson M, Sandström M, Lewsley R, Wennborg A, Abrahmsén L, Tolmachev V and Feldwisch J: Targeting of HER2-expressing tumors using ¹¹¹In-ABY-025, a second-generation affibody molecule with a fundamentally reengineered scaffold. *J Nucl Med* 51: 1131-1138, 2010.